Principal Component Analysis for the characterisation of spatiotemporal variations of the solar resource in urban environments

Guillaume F. J. Le Gall, Martin Thebault, Cyril Caliot, Julien Ramousse

Proceedings of the 17th International Heat Transfer Conference, IHTC-17
14 - 18 August 2023, Cape Town, South Africa

IHTC-17 | ID: 323

PRINCIPAL COMPONENT ANALYSIS FOR THE CHARACTERISATION OF SPATIOTEMPORAL VARIATIONS OF THE SOLAR RESOURCE IN URBAN ENVIRONMENTS

Guillaume Le Gall[1*], Martin Thebault[1], Cyril Caliot[2], Julien Ramousse[1]

[1]LOCIE, Université Savoie Mont Blanc, CNRS, UMR 5271, F-73376 Le Bourget-du-Lac, France
[2]E2S UPPA, LMAP, Université de Pau et des Pays de l'Adour, CNRS, UMR 5142, 1 Allée du Parc Montaury, Anglet, France

ABSTRACT

Urban areas are serious candidates for the production of solar energy but their intrinsic complexity makes it challenging. The heterogeneity in the geometries and radiative properties of the different elements composing the urban fabric, specifically induces important spatiotemporal variations of the distribution of incident solar radiations. Besides, Principal Component Analysis (PCA) has been widely validated as an efficient tool to identify the principal behavioural features of a high-dimensional physical model. This paper proposes a novel approach to analyse and characterise the spatiotemporal variability of the solar resource within an urban context by means of PCA. A theoretical 100×100 m^2 asymmetric urban district made of nine cuboids with various heights is studied. The distribution of the incident field of irradiances is modelled via backward Monte-Carlo ray tracing over a full year on the facets of the central building under a clear sky, with a 15 min timestep and 1 m spatial resolution. PCA is subsequently applied to the simulated model to analyse its spatial and temporal variabilities. First results validate modal decomposition as a powerful technique for the analysis of the variability distribution, allowing the identification of the district areas subjected to important spatial and temporal variations of the solar resource. Characteristic scales are clearly represented by orders of decomposition. The contribution of surrounding geometries is also transcribed by particular spatial modes and similar influential variables are encountered across multiple evaluated surfaces but at different modal ranks.

KEYWORDS: Solar radiations, Urban environment, Spatiotemporal variability, Model Order Reduction, Principal Component Analysis

1. INTRODUCTION

Sunlight is an abundant, inexhaustible and easily accessible natural resource for energy production. Over the last decades, significant efforts have been made to position solar energy as a tangible alternative to traditional non-renewable fuels [1]. If appropriate measures and support policies are being taken and rapidly implemented by governmental authorities, it could be able to meet over 30% of the global energy needs by 2060 [2]. Urban areas are serious candidates for the deployment of solar collectors, since a substantial part of the energy produced is being used directly in cities [3].

However, the complexity of the urban environment makes the production of solar energy challenging. The presence of buildings, vegetation and other obstacles, and the diversity of their geometrical nature

*Corresponding Author: guillaume.le-gall@univ-smb.fr

(e.g., shape, size, orientation and inclination) and materials optical properties (e.g., specular and/or diffuse reflectivity, transmissivity) alter solar and infrared radiative transfers [4]. Multiple reflections of solar radiations and complex dynamic overshadowing effects are taking place between structural elements [3]. Building façades are specifically of important influence here. This participates in the creation of a specific local climate in interaction with the urban infrastructures, contributing to the Urban Heat Island (UHI) effect [5]. Another important agent of solar radiations regulation is the atmosphere itself. Light from the sun passing through the atmosphere is subjected to multiple radiative events (absorption, emission, scattering and reflection) before reaching the ground [4]. This interdependency between the local climate and the urban structure eventually adds on the inherent spatiotemporal variability of the solar resource. The geographic location, daily and seasonal cycles, via the apparent movement of the sun relatively to the Earth, and meteorological conditions, especially through the motion of clouds, are mainly responsible for the natural variations of sunlight. All of this leads to a significant spatiotemporal variability of the solar resource at the urban scale. Various approaches and a plethora of increasingly efficient simulation tools have been proposed for the modelling of radiative exchanges taking place in the urban fabric [3, 6]. However, when dealing with multivariate phenomena involving a huge amount of data over a wide range of spatial and temporal scales, like in the present situation, improvements in the numerical capabilities are still usually not sufficient.

A solution to deal with such complex physical problems is to apply Model Order Reduction (MOR) techniques [7]. MOR has been widely employed in various fields for models defined in high-dimensional spaces (e.g., quantum mechanics, fluid dynamics) or for multiscale problems with very large characteristic spatial or temporal scales (e.g., solid mechanics, acoustics) [8]. In multiple situations, a high-dimensional physical phenomenon can be reasonably approximated by the behaviour of a few numbers of its dominant features [7]. The benefit of MOR in such cases is thus twofold:

1. The essential features are identified, which inherently facilitates the interpretability of the global model's behaviour;
2. The restricted set of features can be used to create a reduced order model of the physical problem and drastically lessen the computational effort for future modelling.

Among the variety of available MOR approaches, Principal Component Analysis (PCA) [9] has been extensively used and validated in multiple areas, including renewable energies [1, 10]. Also known as Principal Orthogonal Decomposition (POD) [11] in computational fluid dynamics, Hotelling Transform [9] and Karhunen-Loève Transform [12] in image processing or the Empirical Orthogonal Function (EOF) [13] in climate science, it consists of identifying the most representative orthogonal features of a given dataset [14], namely directions in which data varies. PCA generates a set of uncorrelated features (principal components) being linear combinations of the original variables and summarising at best the dataset, i.e., accounting for the maximum variance [10]. It is robust to sets of data dealing with multiple interdependent variables and with a high dimensionality with respect to their number of samples [1].

The aim of this paper is to present and investigate the applicability of Model Order Reduction methods as an efficient means to analyse and characterise the spatiotemporal variability of the solar resource within an urban context. In that objective, a numerical simulation of the distribution of annual solar radiations, in terms of irradiances, has first been conducted on a simple theoretical three-dimensional urban geometry of heterogeneous morphology. A subsequent statistical analysis has been performed by means of PCA on the simulated field of irradiances. The main methodology is detailed in section 2. The principal resulting features have finally been analysed with respect to their influence on the model's spatial and temporal variabilities (sections 3 and 4).

2. METHODOLOGY

This section details the methodology and corresponding methods adopted in this work, as well as their underlying rationales and assumptions.

2.1 Numerical model The input geometry has consisted of an assembly of nine three-dimensional buildings, namely one central and eight peripheral structures (Fig. 1). The motive for this configuration was to keep the domain size reasonable for maintaining an acceptable trade-off between speed and accuracy in the simulation process. The main design parameters, i.e., Shape Factor, Floor Area Ratio, Site Coverage and Average Building Height [15], have been defined in the aim of mimicking a theoretical urban district with an open mid-rise typology [16]. The morphological diversity has been restricted here to a heterogeneity in the buildings location and height. They have been arranged in a disorganised manner across the 100×100 m^2 district area and modelled by cuboids of 20×20 m^2 bases with a height ranging from 15 to 35 m. For the sake of simplicity, no semi-transparent (e.g., vegetation) or highly specular (e.g., glazings) elements, which would alter the reflected, transmitted and absorbed components of incoming radiations at the district scale, have been introduced. All surfaces have been considered Lambertian, i.e., perfect diffusers, with a reflectance of 0.3. Thus, both the directional and spectral dependencies of the full geometry on incident radiations have been omitted.

Similar atmospheric profiles to Caliot et al. (2022) [17] have been employed to describe the atmosphere, where the optical properties of its constituting gases are defined using the ECRAD radiation scheme for the European Centre for Medium-Range Weather Forecasts (ECMWF) [18]. No clouds have yet been consider at this stage, resulting in typical clear sky conditions for the location of Paris (48°51′12.28″ N; 2°20′55″ E).

2.2 Annual solar irradiances modelling A new engine, named `htrdr-urban`, has recently been proposed and validated for the accurate simulation of solar and infrared radiative transfers in an urban context with complex geometries and in the presence of a cloudy atmosphere [4, 19]. By combining backward Monte-Carlo ray tracing with Null-Collision Algorithms (NCA), the computational effort becomes quasi-independent of the complexity of the three-dimensional scene. This tool has thus been used here to evaluate

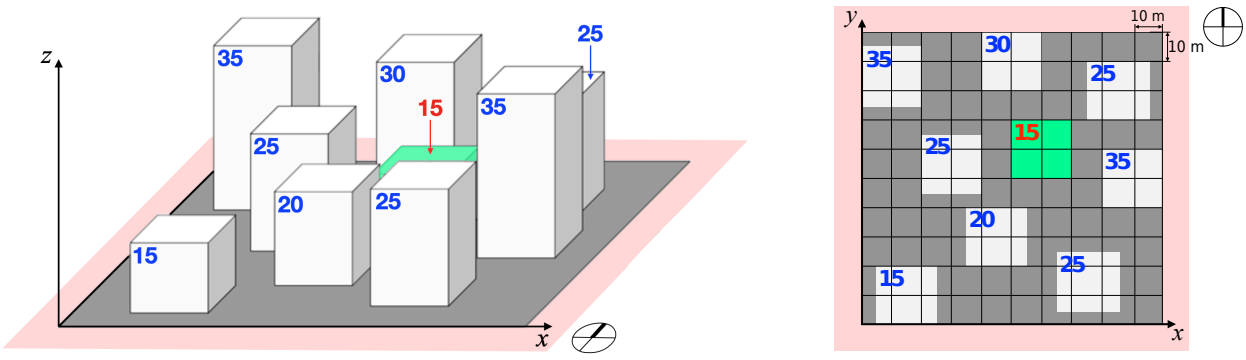

(a) 3D view (b) Top view

Fig. 1 3D (a) and top view (b) of the considered heterogeneous district. Each building is coloured in light grey and referenced in terms of its height (m). The building of interest is highlighted in green. A buffer band of 10 m width surrounds the district area (salmon-pink).

the shortwave irradiances across the measurement grids at each timestep, by solving the monochromatic Radiative Transfer Equation (RTE) for the defined simulation setup. No heat transfers by conduction or convection have been considered, meaning that the simulation boundary conditions at the domain borders are entirely established by the geometry and surfaces albedo of the numerical model.

The simulation has been performed for one building of interest located at the centre of the studied neighbourhood, highlighted in green in Figure 1. The distribution of incident radiations on the considered structure has been evaluated in terms of horizontal or vertical irradiances ($\mathrm{W.m^{-2}}$) for a set of measurement points across its visible surfaces, i.e., for its four vertical façades (east, west, north, south) and roof. Each surface has been discretised into a regular array of points. Similarly to previous studies using the same geometry [6, 20], a spatial resolution of $t_\varphi = 1$ m has been adopted here to allow for a reasonable observation of variations in the spatial patterns of the solar resource. Values have been computed for a full year, from 21$^{\text{st}}$ December 2020, 08:30 to 20$^{\text{th}}$ December 2021, 15:00, with a timestep $t_\alpha = 15$ min.

2.3 Model Order Reduction Principal Component Analysis has been employed to decompose the simulated field of irradiances along its principal features both in the temporal and spatial domains. The rationale behind this decomposition builds on the spatiotemporal separated representation suggested by Pierre Ladevèze a few decades ago [8], by assuming that the incident irradiance distribution on a given surface can be expressed as:

$$E(x,t) = \sum_{k \geq 1} \gamma_k \varphi_k(x) \alpha_k(t) \tag{1}$$

with φ_k and α_k the spatial and temporal contributions, respectively, and γ_k a real number vouching for the field amplitude at rank k. In that aim, the raw dataset of simulated irradiances $E(x,t)$ has initially been arranged in a 2D real matrix of size $n \times p$:

$$\mathbf{E} = \overbrace{\begin{bmatrix} e_{11} & \cdots & e_{1p} \\ \vdots & \ddots & \vdots \\ e_{n1} & \cdots & e_{np} \end{bmatrix}_{n,p}}^{\text{features}} \Bigg\} \text{samples} \tag{2}$$

Its rows (samples) and columns (features) refer to the n annual timesteps and to the p measurement points, respectively. The number of discretisation points being here significantly higher in the temporal than in the spatial domain ($n \gg p$), it results in a very "thin" input matrix $\mathbf{E}$.

When performing PCA, it is a common requirement that data are standardized, i.e., centred around a null mean and scaled to have a standard deviation of one, prior to the reduction procedure. Translating the values by subtracting their means ensures that the first principal component actually reflects the maximum variance of the dataset and not its mean value [14], which would otherwise be likely to make it statistically misleading. Scaling is usually employed to avoid allocating too much weight to some features over the others and reduce noise in the higher-order components [21]. PCA is in that case performed on the correlation instead of the covariance matrix. Within the scope of this work, scaling would not be of high relevancy, since all features are by definition on the same scale. Hence, data centring only has been carried out during the pre-processing stage by deducting to each column j of $\mathbf{E}$ its mean value $\mu_{\alpha,j}$.

PCA can either be performed via Eigenvector Decomposition (EVD) of the covariance (or correlation) matrix for the input data or by applying Singular Value Decomposition (SVD) to the raw dataset directly. In EVD-based PCA, the principal components are accessed via eigenvectors of the covariance matrix (principal directions) and their related amount of information is given by its eigenvalues. When SVD is employed,

the principal directions, i.e., eigenvectors, correspond to the singular vectors of the input matrix, while the singular values are equal to the square root of the eigenvalues (standard deviations). The latter aspect justify why PCA is generally more accurate and numerically robust, yet slightly slower, when based on SVD rather than on EVD for a higher number of samples than features. SVD-based PCA is therefore preferred for high-dimensional datasets [21] and has been used thereafter. Application of SVD to the centred matrix $\dot{\mathbf{E}}$ provides the following decomposition:

$$\dot{\mathbf{E}} = \mathbf{U}.\mathbf{\Sigma}.\mathbf{V}^{\top} \tag{3}$$

with $\mathbf{U}$ a unitary matrix of size $n \times n$ and $\mathbf{\Sigma}$ a $n \times p$ matrix whose main diagonal contains the singular values $\sigma_{\alpha,j}$ associated with the singular vectors represented by the rows of the $p \times p$ matrix $\mathbf{V}^{\top}$ [1]. Having here $n \gg p$, only the first p columns and rows of $\mathbf{U}$ and $\mathbf{\Sigma}$, respectively, related to the p non-null singular values $\sigma_{\alpha,j}$, have been kept to avoid unnecessary huge sizes for these matrices. Equation (3) can thus be rewritten:

$$\dot{\mathbf{E}}' = \mathbf{U}'.\mathbf{\Sigma}'.\mathbf{V}^{\top} \tag{4}$$

where $\mathbf{U}'$ is now of size $n \times p$ and $\mathbf{\Sigma}'$ of size $p \times p$. The principal components, i.e., the projection of the data onto the principal directions, have then been obtained by multiplying $\dot{\mathbf{E}}'$ by $\mathbf{V}$:

$$\dot{\mathbf{E}}'\mathbf{V} = \mathbf{U}'.\mathbf{\Sigma}'.\mathbf{V}^{\top}.\mathbf{V} = \mathbf{U}'\mathbf{\Sigma}' = \begin{bmatrix} \mathbf{pc}_{\alpha,1} & \cdots & \mathbf{pc}_{\alpha,p} \end{bmatrix}_{n,p} \tag{5}$$

with their related variances, i.e., the eigenvalues $\lambda_{\alpha,j}$ of the covariance matrix of $\dot{\mathbf{E}}'$, being directly accessed from the singular values $\sigma_{\alpha,j}$:

$$\lambda_{\alpha,j} = \frac{\sigma_{\alpha,j}^2}{n-1} \tag{6}$$

Finally, the principal component $\mathbf{pc}_{\alpha,j}$ of rank j is simply selected from the columns of $\dot{\mathbf{E}}'\mathbf{V} = \mathbf{U}'\mathbf{\Sigma}'$, while its rows give the samples coordinates in the projection space. To visualise the corresponding mode $\hat{\mathbf{E}}_{\alpha,j}$, i.e., the reconstruction of the original dataset from this principal component only, $\mathbf{pc}_{\alpha,j}$ has further been multiplied by its related principal direction $\mathbf{v}_j^*$ (j-th column in $\mathbf{V}^{\top}$), and its mean value $\mu_{\alpha,j}$ summed back:

$$\hat{\mathbf{E}}_{\alpha,j} = \mathbf{pc}_{\alpha,j}.\mathbf{v}_j^* + \mu_{\alpha,j}\mathbf{I} \tag{7}$$

The above demonstration is valid within the scope of a temporal decomposition, with the n annual timesteps and the p grid points accounting for the samples and the features, respectively, in the PCA calculation. The idea being to investigate both the temporal and spatial variabilities of the field of irradiances, $\mathbf{E}$ has also been transposed so that its rows now depict the p evaluation points (samples) and its columns the n related timesteps (features). The input dataset $\mathbf{E}^{\top}$ for spatial decomposition would thus be a "thick" matrix of size $p \times n$, with $\mu_{\varphi,i}$ the mean values over its temporal features (columns). The role of $\mathbf{U}$ and $\mathbf{V}$ would be reversed with respect to the illustrated case. Though $p \gg n$ in this configuration, the size of the dataset employed within the scope of this work was still reasonable for the SVD procedure to remain fast enough.

The first modes resulting from the temporal ($\hat{\mathbf{E}}_{\alpha,j}$) and spatial ($\hat{\mathbf{E}}_{\varphi,i}$) decompositions have then be examined to assess the variabilities of the incident field of irradiances (section 3).

[1] $\mathbf{V}^{\top}$ refers here to the transpose of the real matrix $\mathbf{V}$

3. RESULTS

Results from the modal decomposition of the incident field of irradiances on the different facets of the test building are presented here. The spatial and temporal decompositions for the first four modes on the east façade (Fig. 2) and for the first modes on each of the orther surfaces, i.e., west, north, south and roof, (Fig. 3) have been selected by the authors for visualisation. Their amplitudes have all been normalised between -1 and 1 and centred around 0 using a diverging colour scale to facilitate the analysis. Only modes up to the fourth rank are investigated, since they capture, by definition, most of the variability (cf. 3.3). It is not excluded that higher order modes account for interesting behaviours, yet they will not be analysed within the scope of this preliminary study.

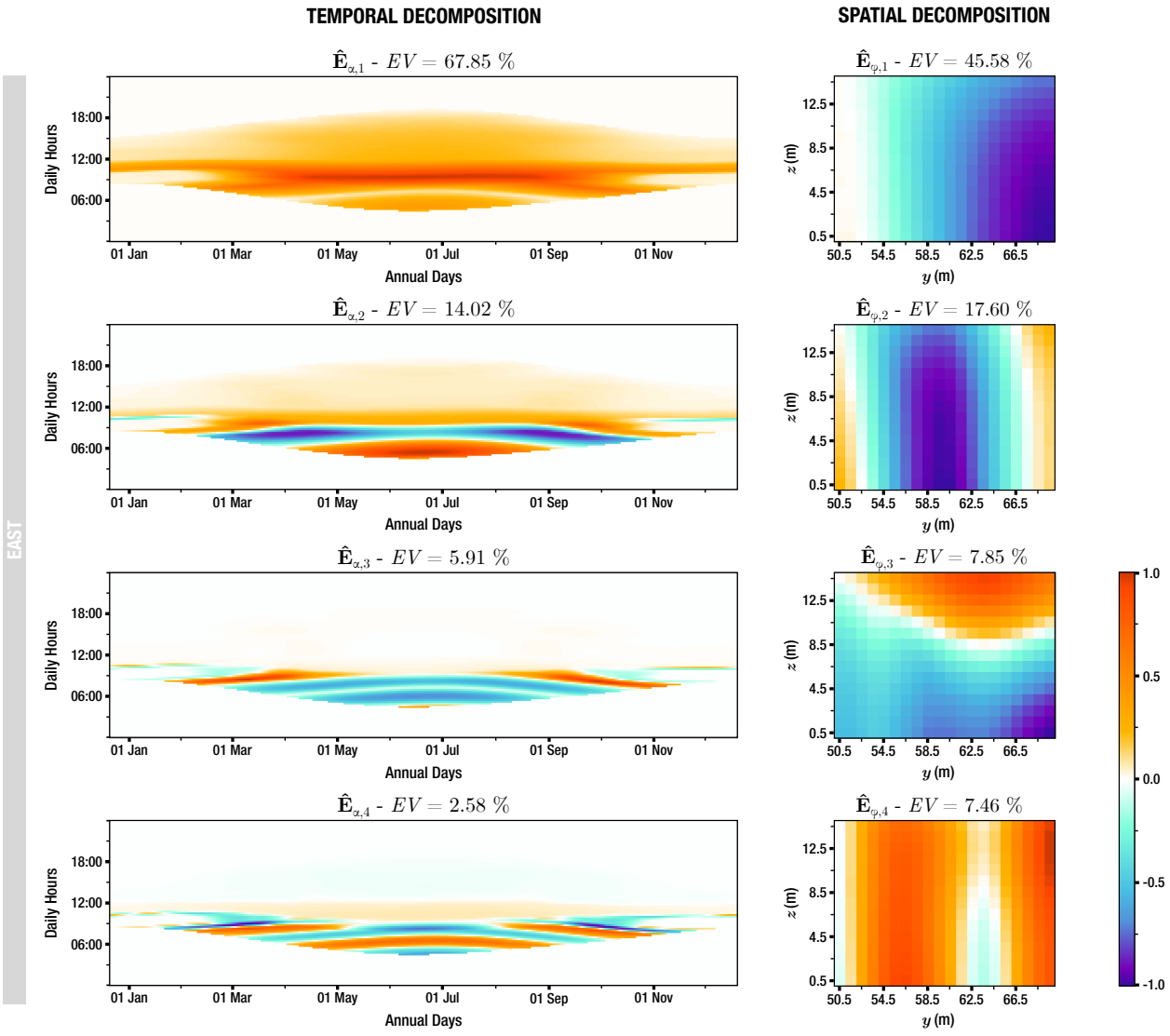

Fig. 2 Temporal (left column) and spatial (right column) decompositions of the incident field of irradiances on the east façade of the test building. The first four modes $\hat{\mathbf{E}}_{1-4}$ are displayed row by row in growing order. Spatial axes are defined with respect to the coordinate system used in Fig. 1.

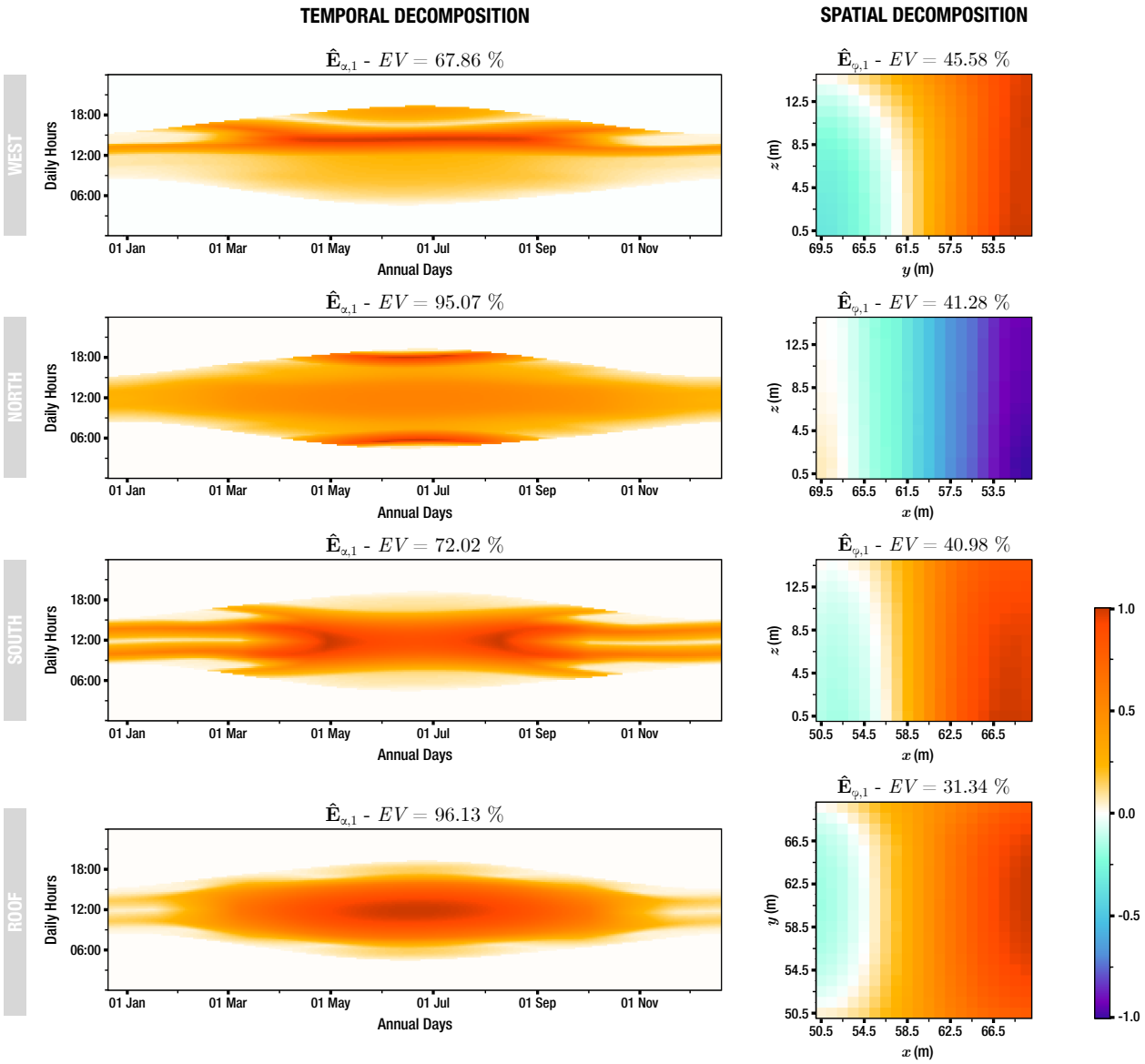

Fig. 3 Temporal (left column) and spatial (right column) decompositions of the incident field of irradiances on the west-, north-, south-facing and roof surfaces of the test building. Only the first modes $\hat{\mathbf{E}}_1$ are displayed here (rows). Spatial axes are defined with respect to the coordinate system used in Fig. 1.

3.1 Temporal decomposition The temporal decomposition for each mode of interest is represented on the left column in Fig. 2 and 3 by the normalised irradiance received at a given time in a day (24 hours) as a function of a speficic day in the year (365 days). As it could have been expected, a first common trend to the temporal modes across the different surfaces is that they depict the variabilities in the distribution of irradiance at different time scales, with the level of details provided by each of them increasing with their order. Namely, $\hat{\mathbf{E}}_{\alpha,1}$, which accounts for the highest explained variance (EV), generally provides information about the global annual irradiance distribution and highlights the seasonal repartition (winter/summer) (Fig. 2, 3 - $\hat{\mathbf{E}}_{\alpha,1}$). Subsequent higher-dimensional modes represent finer variations, from the daily sharing between the morning and the afternoon, including midday in some cases, and up to an explanation at the hour scale (Fig. 2 - $\hat{\mathbf{E}}_{\alpha,2-4}$). $\hat{\mathbf{E}}_{\alpha,4}$ for the east, west and south façades further shows the influence of equinoxes and solstices on the daily irradiance distribution (Fig. 2 - $\hat{\mathbf{E}}_{\alpha,4}$).

Rationally, the distribution for each temporal mode is similar yet symmetric with respect to midday for the east and west façades (Fig. 2, 3). All of the first four dominant modes for both surfaces also share very close respective variances. Similarly, modes for the south and north sides seem to be complementary (Fig. 3), taking into account the daily course of the sun. However, the amount of information is interestingly more concentrated within the first mode for the north than for the south orientation. In general, this trend has been observed across surfaces of different orientations, with notable differences in the explained variances provided by modes of a same decomposition rank k.

3.2 Spatial decomposition The spatial decomposition for the same modes as detailed in section 3.1 is represented on the right column in Fig. 2 and 3 by the normalised irradiance received at a given position on the considered facet. Overall, results for the spatial decomposition correlate with the above observations in the temporal domain. However, more similarities have been found between the spatial distributions of the first dominant modes from the different surfaces. All the first four modes for the east and west façades now depict almost exactly the same allures (not shown here). Their respective explained variances are also very similar and close enough to the values of the corresponding modes for the south façade. The total variance spreads more equally over the four dominant modes here than for the temporal decomposition, the amount of information held by the first mode alone being lower in the present situation (Fig. 3).

Interestingly, similar modal distributions are encountered across multiple vertical surfaces but at different ranks k, e.g., $\hat{\mathbf{E}}_{\varphi,3}$ for the north side is similar to $\hat{\mathbf{E}}_{\varphi,2}$ for the east and west orientations (not shown here).

The influence of surrounding geometries on the distribution of the field of irradiances is more clearly highlighted here. This is especially illustrated by the slight variations in the distributions of modes of same rank k between the east and west surfaces (Fig. 2, 3), which would not have been observed in a completely symmetric area under clear sky conditions. The differences in the heights and positions of neighbouring buildings on the western and eastern sides of the considered structure may have induced these variations.

3.3 Scree Plots Finally, scree plots, which express the explained variance as a function of principal components, have been computed for both the temporal and spatial decompositions for each facet. For all surfaces and domains, it has been observed that a substantial part of the total explained variance is contained in the first few components, i.e., modes. In the case of the east-facing façade, modes after the tenth already account for less than 0.5 % of the total explained variance each (Fig. 4).

4. DISCUSSION & CONCLUSIONS

A novel approach for the analysis of solar radiations variabilities in urban environments by means of Principal Component Analysis has been proposed. The field of irradiances has been simulated onto the façades and roof of a cuboidal building within an urban context of heterogeneous structures. First results show that modal decomposition provides a very efficient tool to analyse the first dominant modes of the variability distribution in both the temporal and spatial domains.

Overall, a reasonable consistency has been observed between results from the temporal and spatial decompositions. Lower-dimensional modes, i.e., with the highest variances, have been found to account for the variations on wide scales while modes at higher ranks describe the variations on smaller scales. In the complex urban environment where a plethora of parameters are likely to play a role in the variability of the solar resource, MOR methods would greatly facilitate the identification of the most influential parameters at characteristic spatiotemporal scales. Especially, the contribution of specific surrounding geometries to the disturbance of the incident field of irradiances has been pinpointed by certain spatial modes. The orientations

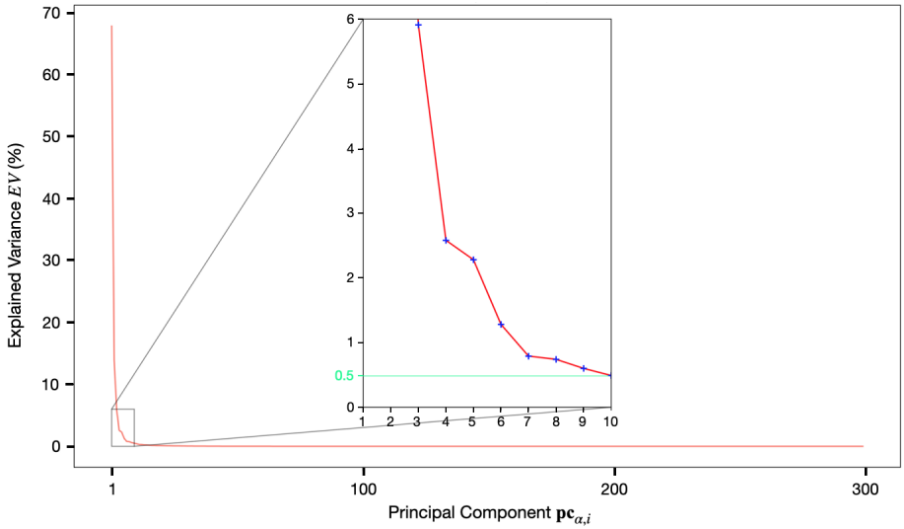

Fig. 4 Scree plot for the temporal decomposition on the east façade of the test building.

of the evaluation surfaces have clearly been represented in the decomposition, with complementarities and/or similarities between facets on the same axes (north/south or east/west). Results for the east- and west-facing façades have presented great consistency across the different decomposition modes. In general, a different amount of information was provided by modes of same dimensions for the north and south façades, and compared to the east/west axis. This suggests that specific characteristic scales contribute more to the global spatiotemporal variations for some orientations than for others. The distribution of certain spatial modes has also been found to be common to several of the vertical surfaces, but at different orders of decomposition. This implies that same parameters are involved in the spatial variability of the field of irradiances across the surfaces, yet to a different extent depending on their orientation. These findings would therefore be of high relevancy to identify areas subjected to high spatial and temporal variabilities of the solar resource.

Scree plots have further shown that the first few principal components were sufficient to capture a significant part of the information in our physical model (above 96.5 % and 84,3 % of cumulative EV held by the first 10 components for the temporal and spatial decompositions, respectively), paving the way for the definition of a reduced order model that would be very close to the original. These results therefore demonstrate that the use of PCA, and MOR methods in a wider extent, can be very promising approaches to analyse the spatiotemporal variabilities of the irradiance field, which would be otherwise very complex given the high spatial and temporal definitions.

This work has led to promising findings but still presents some limitations, which should be pointed out. The main limitation comes from the numerical model itself. The geometry has been defined simple on purpose, with a limited number of variables. The objective was here to validate the applicability and efficiency of MOR methods for the analysis of solar radiations variabilities in a heterogeneous environment. The consideration of more complex (e.g., shapes, inclination of surfaces), diverse (e.g., vegetation) and numerous geometries, with non-trivial reflective properties (e.g., specular, semi-transparent), would have likely impacted the results and the difficulty of their analyses. The influence of clouds has neither been considered, since a simple clear sky model has been used here. Besides, the analysis has been restricted to the first four modes for each orientation. Though the authors have sensibly based their decision from the results of preliminarily computed scree plots, higher-dimensional modes could have provided more insights on specific aspects.

Future suggested work would be therefore to apply the proposed methodology to more complex numerical

models, with geometrical and physical properties closer to a real urban neighbourhood. Especially, the variations in common morphological factors like the domain size or the buildings dimensions and arrangement, which would have an apparent impact on the distribution of incident irradiances, are intended to be investigated by the authors. Non-Lambertian surfaces, e.g., highly specular glazings or semi-transparent materials, are also common features of modern urban environments, and their effect on the incoming radiations is worth being examined via the proposed method. The influence of different sky types should also be explored, to consider the effect of clouds in the simulation of solar radiations (e.g., movement, radiative properties). The spatiotemporal resolutions for the simulation could also be finer, e.g., minutely and sub-meterly in the temporal and spatial domains, respectively. Regarding the modal decomposition, other MOR methods should be investigated. Although the relevancy and efficiency of PCA has been evidenced in this study, other techniques may prove relevant for this specific problem. For instance, Proper Generalized Decomposition (PGD) is based on separated representations, e.g., of space and time, and would therefore be a prime candidate in such situations [8]. Similarly, Dynamic Mode Decomposition (DMD) [22], which could be sensibly apprehended as a combination of PCA and Fourier transform, has been proposed specifically to analyse and capture dynamics of evolving physical fields, e.g., fluid flows [14]. The use of deep neural networks for the selection and extraction of the optimal features is also of current interest [23], though still mainly employed for the post-processing of reduced order models. The nature of the decomposition method remains crucial, as on it depends the meaning of the decomposition modes, so does the underlying physics [14].

ACKNOWLEDGMENT

This work has been supported by the French National Research Agency, through the Investments for Future Program (ref. ANR-18-EURE-0016 – Solar Academy). The research unit LOCIE is member of the INES Solar Academy Research Center.

REFERENCES

[1] García-Cuesta, E., Aler, R., del Pózo-Vázquez, D. and Galván, I. M., "A combination of supervised dimensionality reduction and learning methods to forecast solar radiation", *Applied Intelligence*, Retrieved November 09, 2022 from https://doi.org/10.1007/s10489-022-04175-y (2022).

[2] IEA, "Solar Energy Perspectives", Tech. rep., International Energy Agency (IEA), Paris, Available at https://www.iea.org/reports/solar-energy-perspectives [accessed December 4, 2022] (2011).

[3] Freitas, S., Catita, C., Redweik, P. and Brito, M. C., "Modelling solar potential in the urban environment: State-of-the-art review", *Renewable and Sustainable Energy Reviews*, 41, pp. 915–931, doi:https://doi.org/10.1016/j.rser.2014.08.060 (2015).

[4] Caliot, C., Schoetter, R., Forest, V., Eymet, V. and Chung, T., "Model of Spectral and Directional Radiative Transfer in Complex Urban Canopies with Participating Atmospheres", *Boundary-Layer Meteorology*, Retrieved November 02, 2022 from https://doi.org/10.1007/s10546-022-00750-5 (2022).

[5] Johari, F., Peronato, G., Sadeghian, P., Zhao, X. and Widén, J., "Urban building energy modeling: State of the art and future prospects", *Renewable and Sustainable Energy Reviews*, 128, p. 109902, doi:https://doi.org/10.1016/j.rser.2020.109902 (2020).

[6] Thebault, M., Govehovitch, B., Bouty, K., Caliot, C., Compagnon, R., Desthieux, G., Formolli, M., Giroux-Julien, S., Guillot, V., Herman, E., Kämpf, J. H., Kanters, J., Lobaccaro, G., Ménézo, C., Peronato, G. and Petersen, A. J., "A Comparative Study Of Simulation Tools To Model The Solar Irradiation On Building Façades", *Proceedings of the ISES Solar World Congress 2021, Virtual Conference, 25-29 October*, Freiburg: International Solar Energy Society, SWC2021, doi:https://doi.org/10.18086/swc.2021.38.04 (2021).

[7] Schilders, W. H. A., van der Vorst, H. A. and Rommes, J., *Model Order Reduction: Theory, Research Aspects and Applications*, Berlin: Springer (2008).

[8] Chinesta, F., Ladevèze, P. and Cueto, E., "A Short Review on Model Order Reduction Based on Proper Generalized Decomposition", *Archives of Computational Methods in Engineering*, 18(4), pp. 395–404, doi:https://doi.org/10.1007/s11831-011-9064-7 (2011).

[9] Hotelling, H., "Analysis of a complex of statistical variables into principal components", *Journal of Educational Psychology*, 24(6), pp. 417–441, doi:http://doi.apa.org/getdoi.cfm?doi=10.1037/h0071325 (1933).

[10] García-Hinde, O., Terrén-Serrano, G., Hombrados-Herrera, M. A., Gómez-Verdejo, V., Jiménez-Fernández, S., Casanova-Mateo, C., Sanz-Justo, J., Martínez-Ramón, M. and Salcedo-Sanz, S., "Evaluation of dimensionality reduction methods applied to numerical weather models for solar radiation forecasting", *Engineering Applications of Artificial Intelligence*, 69, pp. 157–167, doi:https://doi.org/10.1016/j.engappai.2017.12.003 (2018).

[11] Berkooz, G., Holmes, P. and Lumley, J. L., "The Proper Orthogonal Decomposition in the analysis of turbulent flows", *Annual Review of Fluid Mechanics*, 25, pp. 539–575 (1993).

[12] Loève, M., *Probability theory II*, New York, NY: Springer, fourth ed. (1978).

[13] Lorenz, E. N., "Empirical orthogonal functions and statistical weather prediction", Tech. Rep. 1, Massachusetts Institute of Technology, Cambridge, MA, Available at https://eapsweb.mit.edu/sites/default/files/Empirical_Orthogonal_Functions_1956.pdf [accessed December 7, 2022] (1956).

[14] Tu, J. H., *Dynamic Mode Decomposition: Theory and Applications*, Ph.D. thesis, Princeton University, Princeton, NJ (2013).

[15] Natanian, J., Aleksandrowicz, O. and Auer, O., "A parametric approach to optimizing urban form, energy balance and environmental quality: The case of Mediterranean districts", *Applied Energy*, 254, p. 113637, doi: https://doi.org/10.1016/j.apenergy.2019.113637 (2019).

[16] Stewart, I. D. and Oke, T., "Local Climate Zones for Urban Temperature Studies", *Bulletin of the American Meteorological Society*, 93, pp. 1879–1900, doi:https://doi.org/10.1175/BAMS-D-11-00019.1 (2012).

[17] Caliot, C., Schoetter, R., Forest, V., Eymet, V. and Chung, T., "Starter Pack and validation scripts for the Monte-Carlo-based urban radiative transfer model described in "Model of Spectral and Directional Radiative Transfer in Complex Urban Canopies with Participating Atmospheres"", [Submitted for publication to Boundary-Layer Meteorology], (1.0.0). Retrieved December 29, 2022 from https://doi.org/10.5281/zenodo.7053385 (2022).

[18] Hogan, R. and A., B., "ECRAD: A new radiation scheme for the IFS", Tech. rep., European Centre for Medium-Range Forecasts (ECMWF), Reading, UK, Available at http://www.ecmwf.int/en/research/publications [accessed February 16, 2023] (2016).

[19] |Méso|Star>, "htrdr", https://www.meso-star.com/projects/htrdr/htrdr.html (2018).

[20] Govehovitch, B., Thebault, M., Bouty, K., Giroux-Julien, S., Peyrol, E., Guillot, V., Ménézo, C. and Desthieux, G., "Numerical Validation of the Radiative Model for the Solar Cadaster Developed for Greater Geneva", *Applied Sciences*, 11(17), p. 8086, doi:https://doi.org/10.3390/app11178086 (2021).

[21] Alexandris, N., Gupta, S. and Koutsias, N., "Remote sensing of burned areas via PCA, Part 1; centering, scaling and EVD vs SVD", *Open Geospatial Data, Software and Standards*, 2(17), pp. 1–11, doi:https://doi.org/10.1186/s40965-017-0028-1 (2017).

[22] Schmid, P. J., "Dynamic mode decomposition of numerical and experimental data", *Journal of Fluid Mechanics*, 656, pp. 5–28, doi:https://doi.org/10.1017/S0022112010001217 (2010).

[23] Higashiyama, K., Fujimoto, Y. and Hayashi, Y., "Feature extraction of numerical weather prediction results toward reliable wind power prediction", *2017 IEEE PES Innovative Smart Grid Technologies Conference Europe (ISGT-Europe), Turin, Italy, 26-29 September*, New York, NY: IEEE, pp. 1–6, doi:https://doi.org/10.1109/ISGTEurope.2017.8260216 (2017).